

Shallow-water coherence of broadband signals

M. Badiey¹, J. Simmen² and X. Tang¹

¹Ocean Acoustics Laboratory
Graduate College of Marine Studies
University of Delaware
Newark, DE 19716-3501, U.S.A

²Ocean Acoustics Program
Office of Naval Research, ONR 321 OA
Arlington, VA 22217-5660, U.S.A

Abstract

The frequency-dependent spatial and temporal variabilities of sound propagation in coastal regions is investigated by experiment and numerical simulations. Experimental observations show that temporal coherence of the propagated broadband signal changes significantly with pulse center-frequency, as well as varying with geographic location and time (i.e., different environments). Numerical simulations of such sound transmissions are carried out by using the full-wave broadband PE model and reasonable agreement with the experimental data is found.

1. Introduction

Sound propagation in shallow-water regions is complicated by multiple interactions of the acoustic waves with the sea bottom and sea surface, in addition to the usual interaction with the water column. The degree to which these different interactions cause degradation in the coherence of the pressure field at some distance is not well understood and depends on the scales of the variability in the water column, sea surface and sea bottom, as well as the frequency of the acoustic signal. Numerical modeling has indicated the importance and interplay of sea surface and bottom roughness alone [1] or of volume fluctuations.

Ocean environment monitoring techniques such as acoustical tomography [2] that exploit the use of acoustics have been practiced in deep water but may work equally as well in shallow water. The success of acoustical tomographic methods in shallow-water environments will be limited by our ability to separate out acoustic fluctuations due to the ocean volume from those due to the sea surface and sea bottom/subbottom. The optimal choice of a signal frequency or waveform to probe shallow-water environments is not obvious and will depend on the goals of the tomographic effort. To address this latter issue, we have initiated a study of the dependence of acoustic fluctuations on signal center-frequency for pulses propagated in shallow water [3]. Our immediate objective is to determine the dependence of coherence for a propagated broadband signal on center-frequency, bandwidth, ray path, and ocean environment. In this paper we present the results from a recent acoustic experiment and, for comparison, from corresponding numerical simulations intended to capture the primary features of the experiment.

2. Experimental Observation

In order to investigate the frequency dependence of broadband signals, several underwater acoustic experiments have been conducted in the last few years at locations where previous oceanographic studies have been conducted. These experiments have been performed primarily at two sites: one is the Atlantic Generating Station (AGS) site off shore New Jersey [4] in waters having a mean depth of approximately 14 m; the other is the Delaware Bay site [3] having a mean water depth of approximately 15 m. Figure 1 presents a general schematic layout of these experiments. To purposely avoid a contribution of instrument motion in the acoustic fluctuations, the source and receiver were mounted on tripods placed on the seafloor. The source-receiver ranges for these experiments varied from approximately 200 to 800 m. Series of M-sequences were transmitted at different center-frequencies

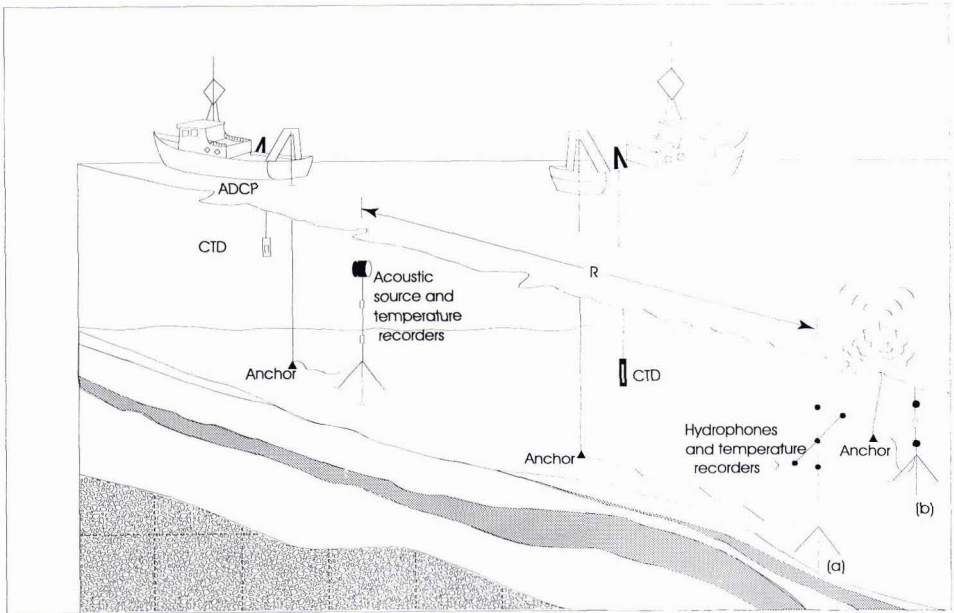


Figure 1: Experimental configuration: (a) Atlantic Generating Station site (range, $R=214$ m) and (b) Delaware Bay site ($R \approx 760$ m).

to allow an easy examination of pulse propagation behavior as a function of frequency. Oceanographic parameters of temperature and salinity were measured by thermistors and CTD's.

In this paper we focus on the analysis for the second experiment which was conducted in the Delaware Bay. For the Delaware Bay site experiments, broadband pulses with variable bandwidths of 0-4 kHz, 0-8 kHz, 5-13 kHz, and 9-25 kHz were used. These bands were chosen to cover the entire low-to-mid frequency spectrum with overlapping coverage. The broadband pulses were filtered to divide the original 4 bands into Gaussian-shaped sub-bands with a fixed bandwidth and center-frequencies ranging from 1-22 kHz. The bandwidths of the lowest frequencies were narrower than those of the higher frequencies to insure that behaviors such as bottom interaction would not be averaged across too wide a band. For example, for 1-2 kHz center frequency the bandwidth was 1 kHz, for 3-6 kHz it was 2 kHz, for 7-11 kHz it was 3 kHz, and for 12-22 kHz the bandwidth was 4 kHz.

The receiver array in the Delaware Bay experiment was tethered to a surface buoy located approximately 760 meters from the source (Fig. 1), and the received acoustic signals were transmitted from the surface buoy to the source ship via VHF radio telemetry. The acoustic source was a F56 transducer with a maximum power of 160 dB re $1 \mu\text{Pa}$ @ 1m (and the average signal to noise ratio for this experiment was 25 dB). This source was tethered to the ship (R/V Cape Henlopen).

Figure 2 shows, for a center-frequency of 2 kHz and geotimes from $T_g=0$ to 12 hours, the received signal amplitude versus time. The solid curves in the figure show the predicted times for the first several groups of arrivals as a function of geotime, based primarily on the changing geometry of ray paths due to tide and secondarily on the advection of sound due to the ocean current. The first peak (i.e., 1) is actually comprised of three interfering arrivals, and subsequent peaks (i.e., 2,3,...) are comprised of pairs of interfering arrivals, corresponding to ray paths having multiple surface and bottom interactions. The three ray paths that comprise the first interfering group, include the direct path, single surface bounce, and surface-bottom bounce. Note how closely as a function of geotime the calculated arrival time tracks the measured arrival time for the first several arriving peaks. The strongest arriving peaks (i.e., 2 - 5) are those immediately following the first peak, followed by peaks (i.e., 6, 7, ...) with noticeably reduced amplitudes, presumably due to the extended interaction with, and attenuation, from the sea surface and bottom.

Figure 3 illustrates the frequency dependence of the received signals. In this figure the received signal amplitude versus arrival time is presented as function of center-frequency for a fixed geotime (i.e., $T_g \approx 5$ hrs). The monotonic

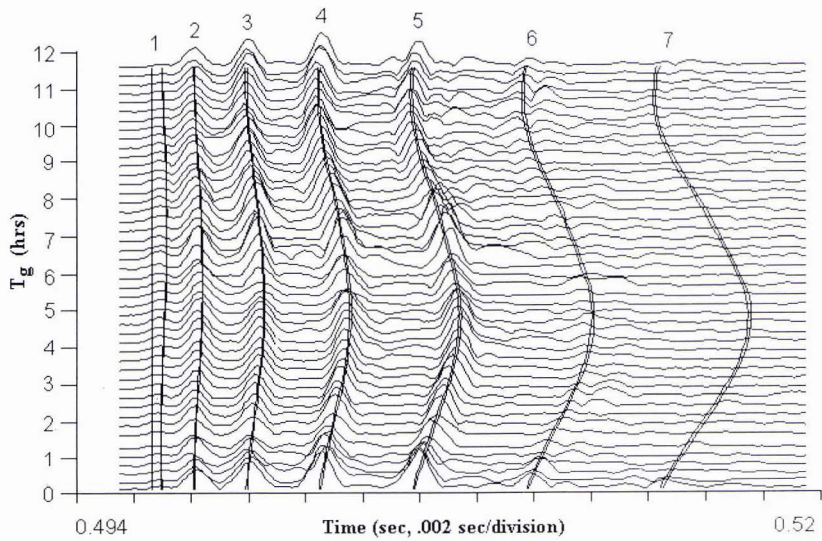


Figure 2: Measured signal amplitude versus time, after correction for source-receiver separation ($f_c = 2$ kHz). The solid lines are predicted arrival times versus geotime, T_g for the first several ray paths.

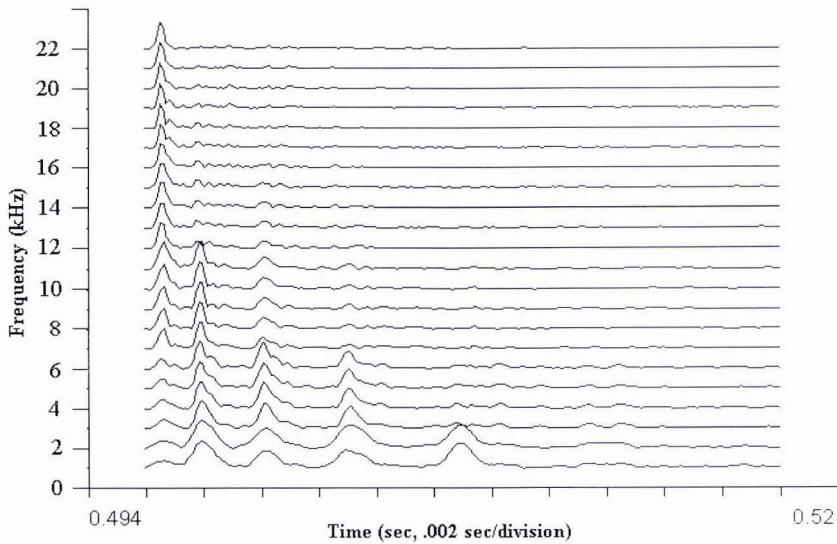


Figure 3: Time series of received signal amplitude as a function of frequency for $T_g \approx 5$ hrs.

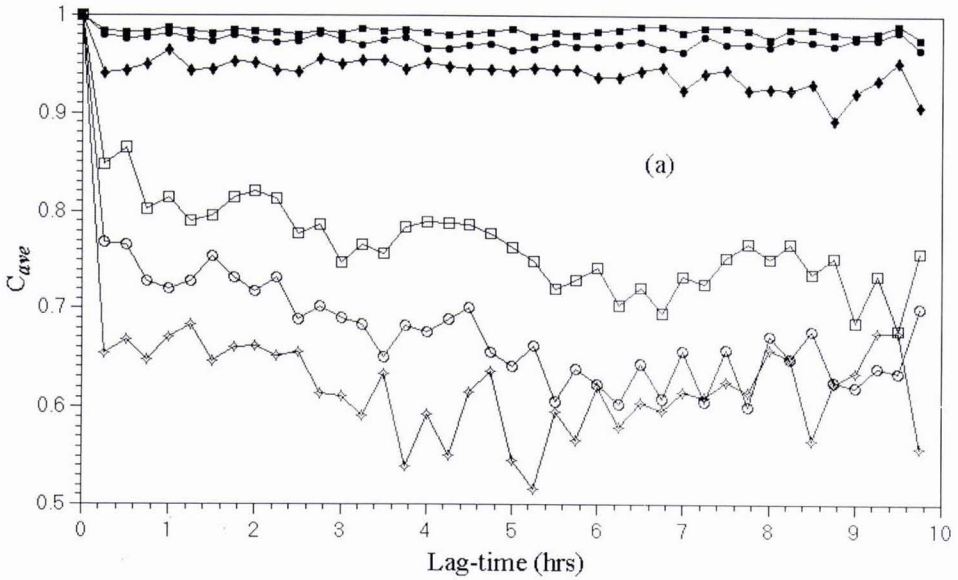


Figure 4: Average correlation for second peak (e.g., number 2 in Fig. 2) versus lag time for $f_c = 2, 4, 9, 12, 15$ and 20 kHz.

growth of the first peak with frequency is a consequence of the fact that a different variable bandwidth filtering and normalization was applied to each frequency. Concealed by this frequency-dependent normalization, the amplitude of all arrivals at high frequencies is much reduced due to attenuation. Figure 3 suggests an inverse law: the number of relatively strong arrivals is approximately inversely proportional to the center-frequency.

In figure 4 the average correlation of the measured signal versus lag time for several center-frequencies and a fixed peak is presented. It clearly shows a rapid decorrelation at higher frequencies, especially those above 9 kHz. For lower center-frequencies there is hardly any decorrelation in signal over several hours, while for signals with the highest center-frequencies there was substantial decorrelation over times as short as 10 to 20 minutes. Generally, the data analysis shows a trend of increasing signal decorrelation (between consecutive pulses) with increasing center-frequency, and increasing signal decorrelation for paths with increasing number of interface interactions. For those paths that multiply interact with the seafloor and sea surface there is an immediate decorrelation for center-frequencies of several kHz and higher. Furthermore, the data shows that at the higher frequencies, the strength of later arrivals seems to be a function of tidal cycle [3].

3. Numerical Simulations

Although the deterministic character of the measured acoustic data can simply be interpreted using the ray diagrams and experimental geometry, to accurately capture the effect of rough surface and rough bottom scattering, full-wave modeling is warranted. At high frequencies rough-surface scattering effects are strong enough that the consequences of these effects on pulse response functions in the time domain are not at all intuitive, and certainly ray-based approaches will fail to capture these frequency-dependent effects. Our modeling approach is to perform numerical simulations using the 2-D, full-wave broadband PE model, based on the efficient split-step Fourier algorithm.

The pulse signal is modeled via the frequency domain by Fourier synthesis of CW results within the frequency band of interest. This gives

$$\tilde{p}(z, r, t) = \int_{f_c - f_B/2}^{f_c + f_B/2} S(f)p(z, r, f)e^{-i2\pi ft} df, \tag{1}$$

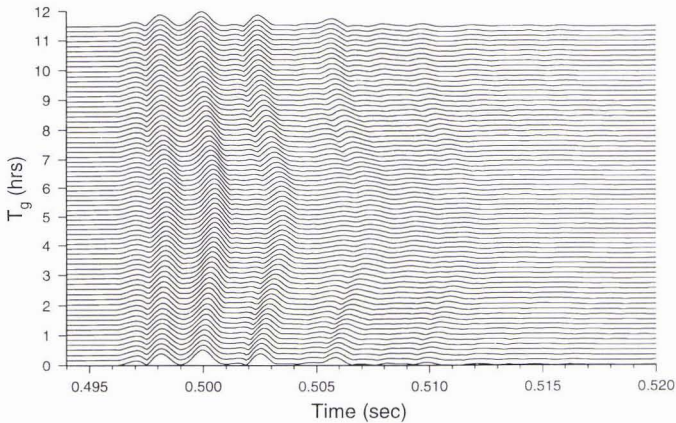


Figure 5: PE-predicted signal amplitude versus time for a rough surface and rough bottom at $f_c = 2$ kHz.

where f_c is the center frequency, f_B is the bandwidth of the signal, and $S(f)$ is the source spectrum. A Hann window filter in frequency domain is applied in order to minimize the artificial sidelobes which show up in the time domain. As in the experimental data, the carrier frequency f_c is eventually removed from the final Fourier synthesis to make for an easy comparison of pulse shapes across frequency. The seafloor was modeled as a fluid with a constant attenuation of 0.2 dB per wavelength. The soundspeed profiles calculated from the measured CTD data are used as input to the model. However, the surface and bottom roughness were not measured during the experiments, so we use numerically generated random boundaries instead. For the sea surface we choose a modified Toba spectrum [5] from which we realize surface roughness, while for the seafloor we choose the Goff-Jordan spectrum [6] to realize the bottom roughness. The validity of these spectra in shallow water is certainly questionable, however, at least they provide a starting point for characterizing interface roughness.

For our experimental geometry, pulse transmissions are numerically simulated with interface roughness added according to these spectra models. In Figure 5, the simulated results of pulse arrivals for the case of a 2 kHz center-frequency are plotted for comparison to Fig. 2. There is a good agreement in the relative amplitudes of peak arrivals between the prediction (Fig. 5) and the actual data (Fig. 2). The numerical calculation confirms that the later peaks (i.e., 6, 7, ...) are noticeably weaker in amplitude than the earlier ones because of energy loss due to multiple bottom interactions at higher grazing angle and that the changing tide significantly influences the strength of the later arriving peaks. In Figure 5 the effects of interface roughness are seen most notably in the later arrivals, where the peaks are less coherent. At higher center-frequencies the simulation shows that the amplitudes of the later arrivals are much weaker and much less coherent due to the enhanced rough surface and bottom scattering and attenuation effects.

4. Summary

In very shallow water regions the temporal coherence for acoustic signals transmitted over several hundred meters is strongly frequency dependent. Above center-frequencies of only a few kHz, we have found significant decorrelation of the signal within a fraction of an hour. There is also a strong dependence of temporal coherence on the ray path or peak arrival. Modeling efforts have begun to account for the stochastic behavior of the ocean, in particular bottom and surface roughness, but before an accurate comparison of the modeled and measured acoustic receptions can be made, measurements of actual interface roughness will be necessary.

5. Acknowledgments

We are thankful to Steve Forsythe for his contributions to several aspects of this investigation. We also wish to thank the efforts of Art Sundberg and the crew of the R/V Cape Henlopen during the experiment.

References

- [1] Rouseff, D., and Ewart, T., "Effect of random sea surface and bottom roughness on propagation in shallow water," *J. Acoust. Soc. Am.*, Vol. 98, No. 6, 3397-3404, 1995.
- [2] Munk, W., Worcester, P., and Wunsch, C., "*Ocean Acoustic Tomography*," Cambridge University Press, N.Y., 1995.
- [3] Badiy, M., Simmen, J., and Forsythe, S. "Frequency dependence of broadband propagation in coastal regions," *J. Acoust. Soc. Am.* 1997 (in press).
- [4] Badiy, M., Jaya, I., and Cheng, A. H-D. "Shallow water acoustic/geoacoustic experiments at the New Jersey Atlantic Generating Station Site," *J. Acoust. Soc. Am.* **96**(6), 3593-3604, 1994.
- [5] Y. Toba, "Stochastic form of the growth of wind waves in a single-parameter representation with physical implications," *Am. Met. Soc.* **8**, 494-507 (1978).
- [6] J. A. Goff and T. H. Jordan, "Stochastic modeling of seafloor morphology: Inversion of Sea Beam data from second-order statistics," *J. Geophys. Res.* **93**, 13589-13609 (1988).